CHINESE OPTICS LETTERS

Vol. 22, No. 2 | February 2024

Constructing arbitrary self-similar Bessel-like beams via transverse-longitudinal mapping

Yanke Li (李岩珂), Yu Zou (邹 昱), Zhaojin Guo (郭兆金), Sheng Liu (刘 圣)*, Peng Li (李 鹏)**, Bingyan Wei (魏冰妍), Dandan Wen (温丹丹), and Jianlin Zhao (赵建林)

Key Laboratory of Light Field Manipulation and Information Acquisition, Ministry of Industry and Information Technology, Shaanxi Key Laboratory of Optical Information Technology, School of Physical Science and Technology, Northwestern Polytechnical University, Xi'an 710129, China

*Corresponding author: shengliu@nwpu.edu.cn

**Corresponding author: pengli@nwpu.edu.cn

Received August 27, 2023 | Accepted October 20, 2023 | Posted Online February 27, 2024

Based on the transverse-longitudinal mapping of Bessel beams, we propose a simple method to construct a self-similar Bessel-like beam whose transverse profile maintains a stretched form during propagation. Specifically, the propagating-variant width of this beam can be flexibly predesigned. We experimentally demonstrate three types of self-similar Bessel-like beams whose width variations are linear, piecewise, and period functions of propagation distance, respectively. The experimental results match well with the theoretical predictions. We also demonstrate that our approach enables the generation of self-similar higher-order vortex Bessel-like beams.

Keywords: Bessel beams; self-similarity; transverse-longitudinal mapping.

DOI: 10.3788/COL202422.022601

1. Introduction

Since the Bessel beam was proposed as an exact solution of propagation-invariant mode to the Helmholz equation[1,2] by Durnin in 1987, it has attracted a great deal of research interest. Due to its properties of nondiffraction and self-healing[3], the Bessel beam has been widely used in the fields of free-space optical interconnects and communications[4,5], optical capture and particle manipulation[6,7], optical micro-nanomachining[8], optical microscopic imaging[9,10], and femtosecond laser processing[11]. In addition, the Bessel beam shows more potential for applications in spatiotemporal light bullets, beam alignment, plasma channels, to name but a few.

Recently, the manipulation of Bessel beams has become an issue of fundamental importance. Many novel behaviors have been developed successively based on the properties of Bessel-like beams. Specifically, employing the transverse-to-longitudinal and spectrum-to-distance mapping of Bessel beams, researchers have proposed some methods to generate Bessel-like beams with propagation-variant polarization[12] or arbitrary trajectories[13–17]. Taking advantage of the dependence of the beam on-axis evolution on the spatial spectrum, it is possible to engineer the axial intensity[18] and polarization[19] of Bessel beams. The linear Gouy phase shift[20] of Bessel beams has also been used to realize propagation-variant polarization[21,22]. In addition, many special structured beams such as helical beams[23–25] have been constructed by superposing multiple Bessel beams.

On the other hand, researchers have also worked to obtain the self-similar solutions of propagating modes in free space, where they can maintain their transverse profiles under specific stretching during propagation. The most two typical examples are Laguerre–Gaussian beams[26] and nondiffracting Bessel beams[1,2]. A few years ago, Xie *et al.* proposed a class of self-similar beams with different scaling factors by solving the paraxial wave equation[27,28]. The exact solutions of self-similar Bessel beams can be acquired, but there are still restrictions on the scaling factors. Recently, Efremidis *et al.* showed the self-similar arbitrary-order Bessel-like beams under tunable stretching transformations based on the Fresnel integral[29]. The related works either have restrictions in scaling factors or require complicated integral calculations.

In this paper, we propose a new method to construct an arbitrary self-similar Bessel-like beam more straightforwardly by employing the transverse-longitudinal mapping. This method enables the predesigning of the beam width during propagation for both zeroth- and higher-order Bessel-like beams by radially tuning the wave vector cone of the Bessel beam. Through experimentation, we observe these self-similar Bessel-like beams with different width-changing functions, and the experimental results meet our expectations. The proposed method is more intuitive and easier to realize and supports the point-to-point controlling of the beam width. It would be of benefit for exploring applications in optical manipulation of microparticles and optical imaging.

2. Theory

Let us start with the general scalar expression for propagation-invariant Bessel fields,

$$U(r,\varphi,z)=\exp(ik_z z)J_m(k_r r)\exp(im\varphi), \tag{1}$$

where (r,φ,z) denotes the cylindrical coordinate, m is the topological charge, and k_r and k_z denote the transverse and longitudinal wave vectors, meeting $k_r^2+k_z^2=k_0^2$ and $k_0=2\pi/\lambda$. In k-space, the wave vector locates on a cone, with the radius and the slant height being k_r and k_0, respectively[30]. We first focus on the case of $m=0$ [i.e., the zeroth-order Bessel mode $J_0(k_r r)$]. The beam width is mainly determined by the transverse wave vector k_r. The full width at half-maximum (FWHM) of the central peak is approximately $W\approx 2.25/k_r$[31]. Thus, k_r can be regarded as the proportion coefficient of the Bessel beam. To generate a self-similar beam of which the beam width is stretched during propagation, it is ideal to change the transverse wave vector along propagation,

$$k_r(z)\approx\frac{2.25}{W(z)}. \tag{2}$$

To freely control the transverse wave vector of a beam during propagation, we can take advantage of the transverse-longitudinal mapping of the Bessel beams[13,32]. Considering that the Bessel beam can be generated by an axicon, we assume that there exists a special axicon segmented by a series of annulus with radius r_i (i is the serial number), each of which has a different apex angle [corresponding to transverse wave vector $k_r(r_i)$], as shown in Fig. 1(a). Light rays from the annulus $(r_i\rightarrow r_{i+1})$ focus to the band (z_i) on the axis and generate a Bessel beam with width $2.25/k_r(r_i)$. If the axicon has a continuously varied apex angle of which the transmission function is expressed by $\exp[-i\Phi(r)]$, the transverse wave vector would become a continuous function of the radial coordinate, and then we would get a Bessel beam with longitudinally varied beam width [see Fig. 1(b)]. Note that the $k_r(z)$ at distance z is determined by $k_r(r)$ at the corresponding radius r on the input plane. There is a one-to-one relationship between the radius r and distance z according to the transverse-longitudinal mapping, meeting

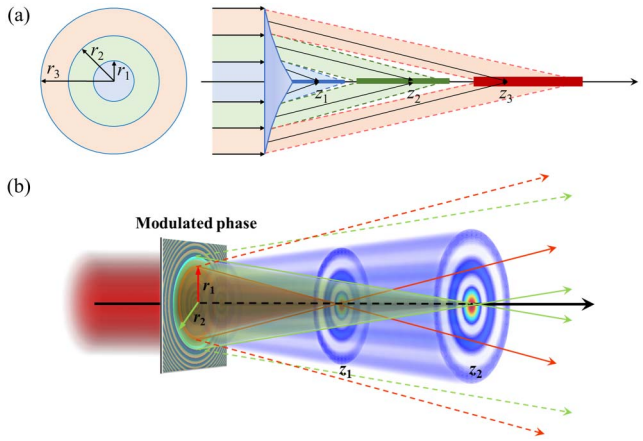

Fig. 1. Schematic of (a) transverse-to-longitudinal mapping of Bessel beam and (b) generation of self-similar Bessel-like beam.

$$\frac{r}{z}=\frac{k_r(r)}{\sqrt{k_0^2-k_r^2(r)}}. \tag{3}$$

By combining Eqs. (2) and (3), we can easily obtain the one-to-one correspondence between the beam width $W(z)$ along the propagation axis and the transverse wave vector distribution $k_r(r)$ at the input plane, while for $k_r(r)$, it denotes the transverse phase gradient, meeting $k_r(r)=\mathrm{d}\Phi(r)/\mathrm{d}r$. Then, we can infer the initial axicon phase $\Phi(r)$ to generate the self-similar Bessel-like beam by the integration

$$\Phi(r)=\int k_r(r)\mathrm{d}r. \tag{4}$$

Thus, the input zeroth-order Bessel-like beam can be expressed as

$$U(r)=J_0[\Phi(r)]. \tag{5}$$

The subsequent self-similar field can be evolved. It is important to point out that the subsequent propagation field at distance z follows the Bessel profile $J_0[k_r(z)r]$, rather than the expression of Eq. (5).

Notably, the precondition of the above one-to-one correspondence is that the rays from the expanding concentric circles cannot intersect with each other. Namely, the focal distance z of the rays from a circle should increase with the circle radius r, meeting $r'(z)>0$. Combined with Eqs. (2) and (3), we obtain a constraint on the beam width function of the self-similar Bessel-like beam,

$$W(z)-zW'(z)>0, \tag{6}$$

which is consistent with the conclusion in Ref. [29]. Moreover, according to the mapping, there is a limitation on the self-similar propagation length due to the finite aperture of the input beam. Theoretically, for a circular aperture R, the propagation length $z_{\max}$ can be given by

$$z_{\max}=\frac{R\sqrt{k_0^2-k_r(R)^2}}{k_r(R)}. \tag{7}$$

3. Results and Discussion

First, we provide a simple example to demonstrate the feasibility of this method. Assuming a linearly varying beam width with $W(z)=Az+B$, Eq. (6) is satisfied as long as $B>0$. The axicon phase can be directly calculated by Eqs. (2)–(4),

$$\Phi(r) = \frac{2.25}{B} r - \frac{Ak_0}{2B} r^2. \tag{8}$$

To verify the self-similar propagation of this beam, we employ the experiment setup containing a spatial light modulator to generate a phase-type hologram, which can encode both the amplitude and the phase into the input beam[33,34]. A collimated linearly polarized laser beam (He–Ne laser, 632.8 nm) is set as the input beam, and the propagation process of the beam is detected in the same way as in our previous work[13].

By setting the parameters $A = 2 \times 10^4$ and $B = 50\,\mu$m in Eq. (8), we demonstrate the zeroth-order Bessel-like beam $J_0[F(r)]$ with linearly varying FWHM as depicted in Fig. 2, where Figs. 2(a) and 2(b) depict the simulated and experimental propagation processes in the x–z plane, respectively. The predesigned beam width is marked by the black dashed lines, which match well with the beam profile. Specifically, the green dashed lines in Fig. 2(a) display the schematic rays to manifest the transverse-to-longitudinal mapping. It can be seen that the angle of the ray decreases during the propagation and produces an increasingly larger spot. Figure 2(c) shows the comparison of the experimentally measured FWHM (error bar) with the predesigned line (red dashed line) and the simulation result (blue dashed line). The experimental data are derived from the average FWHM of four different cross sections, as shown in the inset of Fig. 2(c). From these results, we can see that the experimentally measured FWHM (50–90 μm) has an absolute error of less than 3 μm. This error is acceptable, given the inevitable distortion of the beam profile generated in experiment. Figures 2(d)–2(f) show the intensity cross sections at different propagating distances, referring to the theoretical Bessel mode (red solid lines). They obviously show that the beam maintains classic zeroth-order Bessel modes with the FWHM changes during propagation. These results perfectly represent the self-similar characteristics of the produced beam.

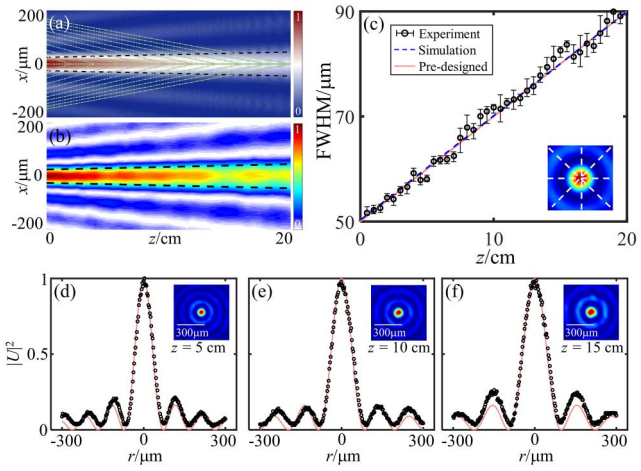

Fig. 2. Propagation process of a zeroth-order Bessel-like beam with linearly varying beam width. (a), (b) Side view of the simulated and experimental propagation process; (c) FWHM versus propagation distance; (d)–(f) intensity cross sections at different propagating distances.

In addition, the transverse-longitudinal mapping of the Bessel beam shows a bigger advantage in controlling the beam width because the points along the propagation axis are independently modulated to a certain extent. This allows for creating an arbitrary function of the beam width variation, including the piecewise function spliced with several different sections. In practical applications, it is essential to obtain a beam with a fixed width and stable propagation. Thus, we can stop changing the beam width after it reaches a certain value, by setting the beam width variation as

$$W(z) = \begin{cases} Az + B & (0 \le z < z_0) \\ Az_0 + B & (z \ge z_0) \end{cases}, \tag{9}$$

where z_0 is the turning point. The corresponding phase can be obtained,

$$\Phi(r) = \begin{cases} \frac{2.25}{B} r - \frac{Ak_0}{2B} r^2 & (0 \le r < r_0) \\ k_{r_0} r + \Phi_{r_0} & (r \ge r_0) \end{cases}, \tag{10}$$

where $k_{r0} = (2.25 - Ak_0 r_0)/B$, $\Phi_{r0} = Ak_0 r_0^2/2B$, and r_0 is given from Eq. (3) by substituting $z = z_0$. In our experiments, we set the parameters $A = 2 \times 10^4$, $B = 50\,\mu$m, and $z_0 = 10$ cm in Eq. (9). Figure 3 presents the experimental results, which carry the same representation as Fig. 2. In Fig. 3(b), the white dashed line marks the turning point z_0. It is observed that the FWHM no longer changes after z_0. Hence, the beam is restored to the nondiffracting Bessel beam $J_0(k_{r0}r)$. Importantly, the nondiffracting distance of this beam is equal to that of the Bessel beam with transverse wave vector k_{r0}. Figure 3(c) shows the measured FWHM, along with the corresponding simulated and theoretical results. These results coincide with each other. Additionally, the beam retains a high-quality Bessel mode during propagation, as illustrated in Figs. 3(d)–3(f).

In theory, the phase $\Phi(r)$ can be calculated by Eqs. (2)–(4) according to the beam width function. However, it is hard to obtain the analytical solutions for a complicated width function $W(z)$. Nevertheless, it is convenient to numerically solve the

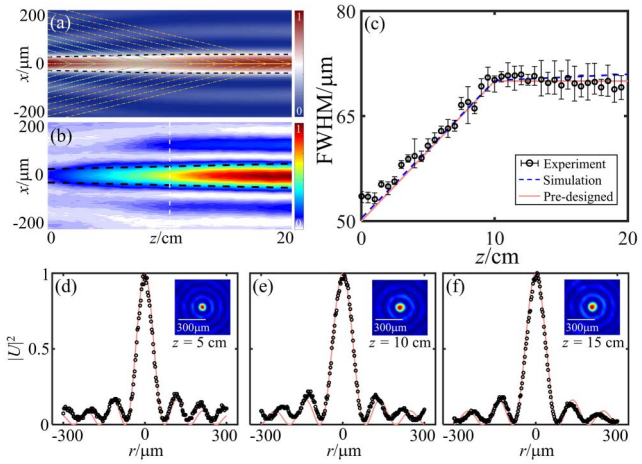

Fig. 3. Same as in Fig. 2 but for piecewise beam width.

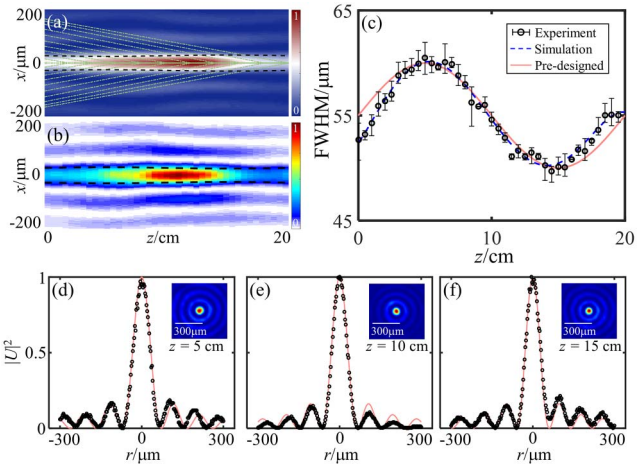

Fig. 4. Same as in Fig. 3 but for sinusoidal beam width.

phase. Here, we select a typical sinusoidal function $W(z)=A\sin(2\pi z/T)+B$, which represents an oscillated beam width. According to Eq. (6), this type of self-similar beam is only valid within some distance. According to Eq. (6), there is an upper limit on the amplitude A of the sinusoidal width. For instance, for given $T=20$ cm and $B=55$ μm, the beam width should be less than $A_{\max}=8.75$ μm to guarantee the stable propagation in one period. Considering the edge diffraction effect, we conduct our investigations on the oscillated self-similar beam by setting $A=5$ μm, $T=20$ cm, and $B=55$ μm. The theoretical and experimental results are shown in Fig. 4. The variation of the FWHM of the beam basically follows the theoretical and simulated curves during propagation. Even though there are some local deviations, the beam width follows a sinusoidal variation overall. Notably, the simulated result also deviates from the ideal sinusoidal curve [see Fig. 4(c)], of which the maximum relative error is ~4.5%. This indicates that a more complicated beam width variation has a larger error caused by the nonlinearity of the transverse-longitudinal mapping. In specific calculations, we improve the computing accuracy, and obtain similar simulated results, while the errors still are inevitable. Additionally, as shown in Figs. 4(d)–4(f), the intensity cross sections at different propagating distances demonstrate that the produced beam can persist with the Bessel profile during propagation. Note that the beam width oscillation is only shown in one period. To achieve the oscillated beam width at a longer distance, we need increase the parameters T or B, or reduce A, according to Eq. (6).

Finally, we show that the proposed method of constructing a self-similar beam is applicable not only for zeroth-order Bessel beams ($m=0$), but also for higher-order ones ($m\neq 0$). Thus, we can generate a vortex Bessel-like beam with any integer order and adjustable beam width. Specifically, for a vortex Bessel-like beam, the beam width can be expressed as the radius of the first ring lobe (i.e., the distance from the origin to the location of the peak intensity) described by $W(z)=X_m/k_r(z)$. Here, X_m is a proportional coefficient determined by the order of the Bessel function m. Generally, $X_1=1.841$, $X_2=3.054$, and $X_3=4.201$. We experimentally demonstrate first- to third-order self-similar vortex Bessel-like beams $J_m[F(r)]$ with a sinusoidally varied beam width. The variation functions of the beam widths are

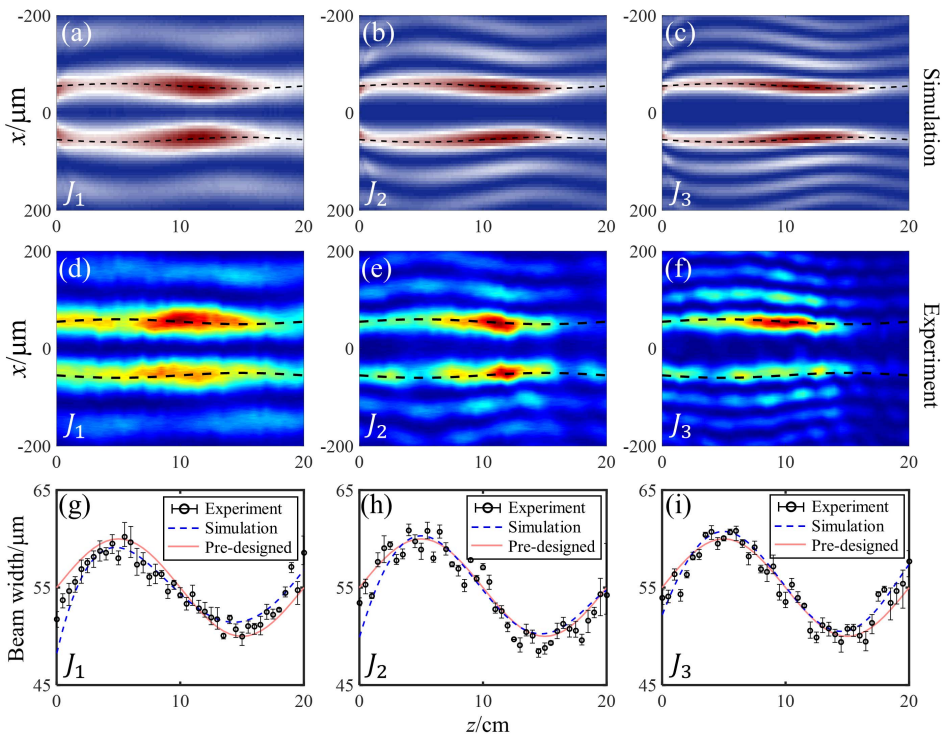

Fig. 5. Propagation process of first- to third-order self-similar vortex Bessel-like beams with sinusoidally varied beam width; (a)–(f) side view of the simulated and experimental propagation process; (g)–(i) corresponding beam width versus propagation distance.

identical to that in Fig. 4. The corresponding phases $\Phi(r)$ are calculated with Eqs. (2)–(4), but replacing 2.25 by X_m in Eq. (2). The simulated and experimental results are shown in Fig. 5 and are basically consistent with the theory. Notably, the asymmetry intensity profile of the experimental results is attributed to the errors of the experimental system arising from generation and detection. Yet the measured beam width [see Figs. 5(g)–5(i)] coincides well with the theory.

4. Conclusion

In conclusion, based on transverse-longitudinal mapping, we show the generation of self-similar Bessel-like beams of arbitrary orders with tunable stretching profiles during propagation and the constraint on the beam width function. We experimentally demonstrate three types of typical self-similar Bessel-like beams with width variations that can be described by linear, piecewise, and periodic functions of propagation distance, respectively. The experimental results match well with the theoretical predictions when the beam width function satisfies the constraint. The proposed approach also enables the generation of self-similar higher-order vortex Bessel-like beams. We expect the proposed method can be also applicable to other nondiffraction beams containing the conical wave vector. The above results would be of benefit for exploring applications in optical manipulation of microparticles and optical imaging.

Acknowledgements

This work was supported by the National Key Research and Development Program of China (No. 2022YFA1404800), the National Natural Science Foundation of China (Nos. 12074312, 12174309, 12074313, and 62175200), and the Fundamental Research Funds for the Central Universities (No. 3102019JC008).

References

1. J. Durnin, "Exact-solutions for nondiffracting beams. I. The scalar theory," J. Opt. Soc. Am. A **4**, 651 (1987).
2. J. Durnin, J. Miceli, and J. H. Eberly, "Diffraction-free beams," Phys. Rev. Lett. **58**, 1499 (1987).
3. Z. Bouchal, J. Wagner, and M. Chlup, "Self-reconstruction of a distorted nondiffracting beam," Opt. Commun. **151**, 207 (1998).
4. R. P. MacDonald, S. A. Boothroyd, T. Okamoto, *et al.*, "Interboard optical data distribution by bessel beam shadowing," Opt. Commun. **122**, 169 (1996).
5. C. Y. Yu, M. R. Wang, A. J. Varela, *et al.*, "High-density non-diffracting beam array for optical interconnection," Opt. Commun. **177**, 369 (2000).
6. V. Garces-Chavez, D. McGloin, H. Melville, *et al.*, "Simultaneous micromanipulation in multiple planes using a self-reconstructing light beam," Nature **419**, 145 (2002).
7. J. Arlt, V. Garces-Chavez, W. Sibbett, *et al.*, "Optical micromanipulation using a Bessel light beam," Opt. Commun. **197**, 239 (2001).
8. E. McLeod and C. B. Arnold, "Subwavelength direct-write nanopatterning using optically trapped microspheres," Nat. Nanotechnol. **3**, 413 (2008).
9. F. O. Fahrbach, P. Simon, and A. Rohrbach, "Microscopy with self-reconstructing beams," Nat. Photonics **4**, 780 (2010).
10. F. O. Fahrbach and A. Rohrbach, "Propagation stability of self-reconstructing Bessel beams enables contrast-enhanced imaging in thick media," Nat. Commun. **3**, 632 (2012).
11. F. Courvoisier, P. A. Lacourt, M. Jacquot, *et al.*, "Surface nanoprocessing with nondiffracting femtosecond Bessel beams," Opt. Lett. **34**, 3163 (2009).
12. I. Moreno, J. A. Davis, M. M. Sanchez-Lopez, *et al.*, "Nondiffracting Bessel beams with polarization state that varies with propagation distance," Opt. Lett. **40**, 5451 (2015).
13. Y. K. Li, S. X. Qi, Y. Q. Xie, *et al.*, "Flexible trajectory control of Bessel beams with pure phase modulation," Opt. Express **30**, 25661 (2022).
14. J. Rosen and A. Yariv, "Snake beam-a paraxial arbitrary focal line," Opt. Lett. **20**, 2042 (1995).
15. V. Jarutis, A. Matijosius, P. Di Trapani, *et al.*, "Spiraling zero-order Bessel beam," Opt. Lett. **34**, 2129 (2009).
16. Y. Hu, D. Bongiovanni, Z. Chen, *et al.*, "Periodic self-accelerating beams by combined phase and amplitude modulation in the Fourier space," Opt. Lett. **38**, 3387 (2013).
17. J. Zhao, P. Zhang, D. Deng, *et al.*, "Observation of self-accelerating Bessel-like optical beams along arbitrary trajectories," Opt. Lett. **38**, 498 (2013).
18. T. Čižmár and K. Dholakia, "Tunable Bessel light modes: engineering the axial propagation," Opt. Express **17**, 15558 (2009).
19. P. Li, Y. Zhang, S. Liu, *et al.*, "Quasi-Bessel beams with longitudinally varying polarization state generated by employing spectrum engineering," Opt. Lett. **41**, 4811 (2016).
20. P. Martelli, M. Tacca, A. Gatto, *et al.*, "Gouy phase shift in nondiffracting Bessel beams," Opt. Express **18**, 7108 (2010).
21. S. Liu, S. X. Qi, P. Li, *et al.*, "Analogous optical activity in free space using a single Pancharatnam-Berry phase element," Laser Photonics Rev. **16**, 2100291 (2022).
22. P. Li, X. H. Fan, D. J. Wu, *et al.*, "Self-accelerated optical activity in free space induced by the Gouy phase," Photonics Res. **8**, 475 (2020).
23. C. Vetter, T. Eichelkraut, M. Ornigotti, *et al.*, "Generalized radially self-accelerating helicon beams," Phys. Rev. Lett. **113**, 183901 (2014).
24. C. Vetter, T. Eichelkraut, M. Ornigotti, *et al.*, "Optimization and control of two-component radially self-accelerating beams," Appl. Phys. Lett. **107**, 211104 (2015).
25. H. Cheng, P. Golvari, C. Xia, *et al.*, "High-throughput microfabrication of axially tunable helices," Photonics Res. **10**, 303 (2022).
26. A. E. Siegman, "Hermite–Gaussian functions of complex argument as optical-beam eigenfunctions," J. Opt. Soc. Am. **63**, 1093 (1973).
27. N. Gao and C. Xie, "Parabolic scaling beams," Opt. Lett. **39**, 3619 (2014).
28. N. Gao and C. Xie, "Free space self-similar beams," Opt. Lett. **40**, 1216 (2015).
29. M. Goutsoulas, D. Bongiovanni, D. H. Li, *et al.*, "Tunable self-similar Bessel-like beams of arbitrary order," Opt. Lett. **45**, 1830 (2020).
30. D. McGloin and K. Dholakia, "Bessel beams: diffraction in a new light," Contemp. Phys. **46**, 15 (2005).
31. J. Turunen and A. T. Friberg, "Propagation-invariant optical fields," Prog. Opt. **54**, 1 (2010).
32. S. Liu, S. X. Qi, Y. K. Li, *et al.*, "Controllable oscillated spin Hall effect of Bessel beam realized by liquid crystal Pancharatnam-Berry phase elements," Light Sci. Appl. **11**, 219 (2022).
33. W. H. Lee, "Binary computer-generated holograms," Appl. Opt. **18**, 3661 (1979).
34. J. A. Davis, D. M. Cottrell, J. Campos, *et al.*, "Encoding amplitude information onto phase-only filters," Appl. Opt. **38**, 5004 (1999).